The Egyptian Journal of Radiology and Nuclear Medicine (2013) **44**, 779–789

Egyptian Society of Radiology and Nuclear Medicine

The Egyptian Journal of Radiology and Nuclear Medicine

www.elsevier.com/locate/ejrnm
www.sciencedirect.com

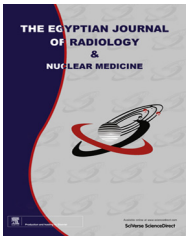

ORIGINAL ARTICLE

The diagnostic performance of chest ultrasonography in the up-to-date work-up of the critical care setting

Rania Refaat *, **Laila A. Abdurrahman**

Department of Radiodiagnosis, Ain Shams University, Cairo, Egypt

Received 30 June 2013; accepted 9 September 2013
Available online 14 October 2013

KEYWORDS

Chest ultrasonography (US);
Chest computed tomography (CT);
Intensive care unit (ICU);
Pulmonary abnormalities;
Pleural abnormalities

Abstract *Background:* Management of patients in the critical care setting is crucial. The availability, the absence of ionizing radiation and the non invasive nature of chest ultrasonography (US) have currently increased its use in the up-to-date work-up of various pleuropulmonary abnormalities in the critical care setting.
Objective: To evaluate the sensitivity, specificity and diagnostic accuracy of chest US for various pleuropulmonary abnormalities in intensive care unit (ICU) patients.
Materials and methods: Ninety consecutive patients admitted in chest ICU with respiratory distress were assessed clinically and by chest radiography (CXR). They were suspected to have a provisional diagnosis of any of the following pathological entities: pneumonic consolidation, bronchogenic carcinoma, metastatic pulmonary nodules, pleural effusion, pneumothorax, hydropneumothorax and mesothelioma. These patients were scheduled for chest computed tomography (CT) and prospectively reviewed using chest US. The results of chest US were compared with these of chest CT for each encountered pathological entity using chest CT as the diagnostic standard of reference to subsequently calculate the sensitivity, specificity and diagnostic accuracy of chest US.
Results: The sensitivity, specificity and diagnostic accuracy of chest US were 100%, 96% and 97% for pneumonic consolidation, 71%, 100% and 98% for bronchogenic carcinoma and 92%, 100% and 99% for pneumothorax respectively. The sensitivity, specificity and diagnostic accuracy of 100% for the rest of the included pathological entities were obtained.
Conclusion: Chest ultrasonography has a considerable diagnostic performance for various pleuropulmonary pathological conditions that may be encountered in the ICU patients making it as an adjunct tool in the up-to-date work-up of the ICU setting.

* Corresponding author. Mobile: +2 01005285089.
E-mail address: raniarefaat_1977@hotmail.com (R. Refaat).
Peer review under responsibility of Egyptian Society of Radiology and Nuclear Medicine.

Production and hosting by Elsevier

0378-603X © 2013 Production and hosting by Elsevier B.V. on behalf of Egyptian Society of Radiology and Nuclear Medicine.
Open access under CC BY-NC-ND license. http://dx.doi.org/10.1016/j.ejrnm.2013.09.001

1. Introduction

Management of critically ill patients requires imaging techniques which are essential for optimizing diagnostic and therapeutic procedures (1). Chest diagnostic imaging is essential when dealing with a critically ill patient (2). Chest computed tomography (CT) is the gold standard for lung imaging; however, it cannot be performed on a routine basis (3). As well, chest CT requires patients to be transported out of the intensive care unit (ICU) putting them at risk of adverse events (4). In addition to the transportation of critically ill patients to the radiology department, the radiation exposure carries a measurable risk (3).

Nowadays, chest ultrasonography (US) is increasingly used in patients managed in the intensive care units (1,5). Moreover, US is a readily available non invasive imaging technique (6) and is useful in imaging lung consolidation, pleural-based masses, pleural effusions and pneumothorax (7). Therefore, there is growing enthusiasm for the use of US providing more immediate, point-of-care imaging (8).

Accordingly, we included various pathological entities so as to investigate the diagnostic performance of chest US, as a bedside tool devoid of ionizing radiation and offering immediate results, in critically ill patients with wide spectrum of pleuropulmonary abnormalities that may be encountered in the ICU setting. We did not take chest radiography (CXR) purposely into account primarily to assess the sensitivity, specificity and diagnostic accuracy of chest US as an individual variable for the detection of various pathological abnormalities in a group of intensive care unit (ICU) patients using chest CT as the diagnostic standard of reference. Secondarily, some CXR are inherently of suboptimal diagnostic capability for ICU patients as they are portable supine radiographs, hence, of poor quality and of low sensitivity.

2. Materials and methods

2.1. Patients

This is a prospective study conducted from August 2012 to March 2013 in which 90 consecutive patients were enrolled. They were admitted in chest ICU with respiratory failure and were assessed clinically and by CXR. The eligibility criteria included provisional diagnosis of any of the following pathological entities: pneumonic consolidation, bronchogenic carcinoma, metastatic pulmonary nodules, pleural effusion, pneumothorax, hydropneumothorax and mesothelioma. These patients were also scheduled for postcontrast chest CT for further appraisal of the provisional diagnoses made. The previously mentioned diagnoses for patient's selection were purposely designed to cover a wide spectrum of the encountered abnormalities. We also aimed to investigate these various abnormalities in the ICU setting to show up the diagnostic performance of chest US as an adjunct tool in the up-to-date work-up for these critical patients. On the other hand, patients having contraindications for postcontrast chest MDCT (renal failure and/or allergy to iodine contrast) and those with hazardous transportation to CT unit were excluded from our study.

Our study protocol was approved by the Committee of Ethics. The patients included in our study underwent chest US and chest CT with a time interval of 24 h. They were included in the order they showed up. Informed written consents were obtained by patients themselves or by their relatives.

2.2. Multiple detector computed tomography (MDCT)

MDCT was performed with a GE Brightspeed Edge Select (8 Slice CT scanner). Scans were obtained in the supine position from the apex of the thorax to the lung bases. MDCT scans were evaluated for pulmonary abnormalities (pneumonic consolidation, metastatic pulmonary nodules, bronchogenic carcinoma and atelectasis) and pleural abnormalities (pleural effusion, pneumothorax hydropneumothorax and mesotheli-

Table 2 Patients' characteristics including age, sex and the encountered pathological entities with the patients' number for each entity.

Age (years)	Mean age: 50 years; age range: 45–65 years
Sex (male patients' number/female patients' number)	55/35
Pneumonic consolidation	16
Bronchogenic carcinoma	7
Metastatic pulmonary nodules	6
Pleural effusion	36
Pneumothorax	12
Hydropneumothorax	6
Mesothelioma	7

Table 1 Differential diagnostic criteria of chest US for distinguishing pneumonic consolidation, peripheral bronchogenic carcinoma and compressive atelectasis [Quoted from (12)].

	Pneumonic consolidation	Peripheral bronchogenic carcinoma	Compressive atelectasis
Echogenicity	Hypoechoic	Hypoechoic	Moderately echogenic
Echotexture	Non homogenous	Mostly homogenous	Mostly non homogenous
Shape	Irregular	Rounded or polycyclic	Concave
Border	Serrated margin	Infiltrating growth	Sharp and smooth
Air bronchogram	A regular feature	None	Often
Characteristic features	Fluid bronchogram may be visible	A single tissue necrosis may occur	Associated with large effusion and a breath- and heart beat-dependent motion within the effusion

Table 3 Sensitivity, specificity, positive and negative predictive values and diagnostic accuracy of chest US compared to chest CT for each encountered pathological entity. True positive (TP), true negative (TN), false positive (FP), false negative (FN).

Pathological entitty	Chest US	Chest CT + ve	Chest CT -ve	Sensitivity (%)[a]	Specificity (%)[b]	PPV (%)[c]	NPV (%)[d]	DA (%)[e]
Pneumonic consolidation	+	16	3					
	–	0	71	100	96	84	100	97
Bronchogenic carcinoma	+	5	0					
	–	2	83	71	100	100	98	98
Metastatic pulmonary nodules	+	6	0					
	–	0	84	100	100	100	100	100
Pleural effusion	+	36	0					
	–	0	54	100	100	100	100	100
Pneumothorax	+	11	0					
	–	1	78	92	100	100	99	99
Hydropneumothorax	+	6	0					
	–	0	84	100	100	100	100	100
Mesothelioma	+	7	0					
	–	0	83	100	100	100	100	100

[a] Sensitivity = $[TP/(TP + FN)] \times 100$
[b] Specificity = $[TN/(TN + FP)] \times 100$
[c] Positive predictive value (PPV) = $[TP/(TP + FP)] \times 100$
[d] Negative predictive value (NPV) = $[TN/(TN + FN)] \times 100$
[e] Diagnostic accuracy (DA) = $[(TP + TN)/(TP + TN + FP + FN)] \times 100$

oma). Each lesion was analyzed according to its number, location, size, borders and CT density. The radiologist who studied chest MDCT images has more than 10 years of experience and was unaware of chest US findings. In this study, we adopted the terminology of the abnormalities detected by chest MDCT as described by the Nomenclature Committee of the Fleischner Society (9).

2.3. Chest ultrasonography

Chest US was performed by the other radiologist who has more than 7 years of experience and was attentive of the patient's clinical history, however, unbiased to chest MDCT. Chest US was performed using Shenzhen mindray DP-1100 plus (China) with a linear array 7.5–10 MHz transducer, curved array 3.5 MHz transducer and a real-time apparatus with gray-scale (B-mode) and time-motion mode (M-mode). The anterior surface of each lung was defined by clavicle, parasternal, anterior axillary line and diaphragm, whereas, the posterior lung surface was defined by the posterior axillary and the paravertebral lines. On the other hand, the lateral surface was defined by the anterior and posterior axillary lines. Each surface was divided into an upper and lower area.

The apex was scanned from the supraclavicular space. Patients were examined in the supine position and in the lateral position to examine the posterior lung surface using longitudinal and transverse scans to all intercostal spaces bilaterally from the base of the lung to the apex of the chest cavity. Examination of patients in the upright (sitting) position was used whenever possible. Identification of normal lung was done as the normal lung generates lung sliding and "A-lines" (repetition lines parallel to the pleural line) (5). These are in addition to demonstration of the "seashore sign" on M-mode (the granular pattern of the respirophasic movement that underlies the horizontal motionless layers of the chest wall and the equivalent of lung sliding in B-mode) (10) and B-lines which are also

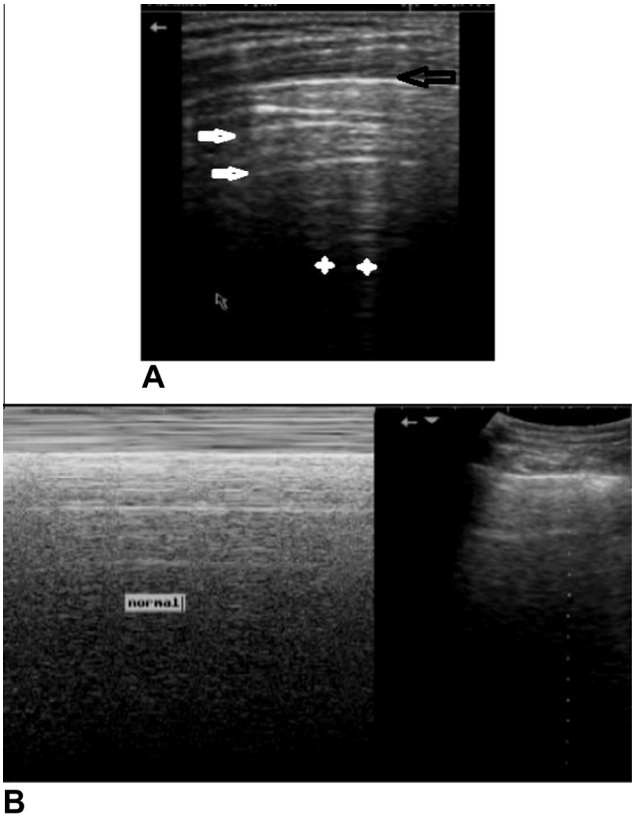

Fig. 1 (A) Chest US image in B-mode shows A-lines (white arrows) and B-lines (asterisks). A-lines (white arrows) are seen as multiple horizontal echogenic lines which are parallel and deep to the pleural line (black arrow). Whereas, B-lines (asterisks) are seen as vertical hyperechoic, narrow-based bands originating immediately below the bright pleural reflection and extending to the lower edge of the image. (B) Chest US image in M-mode displays the typical so-called "seashore" sign which is consistent with the normal lung sliding seen as a homogenous granular pattern below the pleural line.

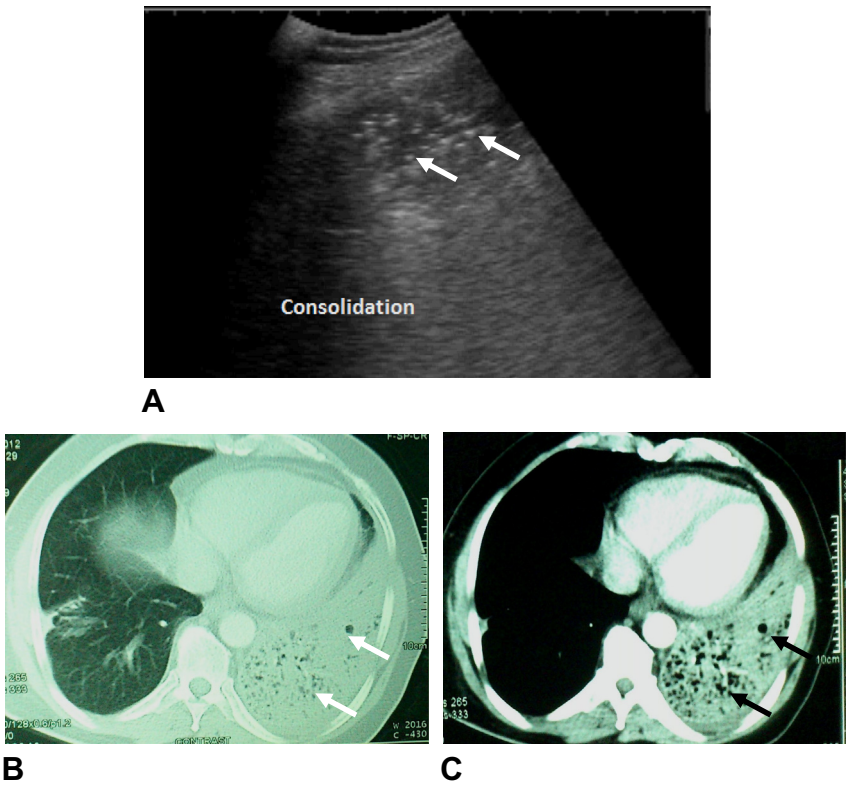

Fig. 2 (A) Chest US image in B-mode displays lung consolidation (showing echogenicity similar to that of the liver) which contains multiple punctiform echogenic foci of air bronchogram inside (arrowed). The air bronchogram is nicely demonstrated as noted in the following CT images. (B and C) Postcontrast chest CT axial images in lung (B) and mediastinal (C) window settings display a consolidative process involving the left lower lung lobe with clearly seen air bronchogram (arrowed).

called "comet tails" or "lung rockets" (one or more mobile vertically orientated lines that originate at the pleural interface) (11).

2.4. The descriptive terms of the chest abnormalities concerned in this study using chest ultrasonography are as follows

Consolidated lung was diagnosed when it has echogenicity similar to that of the liver (11). The sonographic appearance of pneumonia was made on basis of parenchymal and pleural criteria. Regarding the parenchymal criteria, they include hypoechoic area of variable size and shape with irregular and serrated margins and a heterogeneous echotexture with air bronchogram (multiple lentil-sized air inlets of few millimeters in diameter or a tree-shaped echogenic structure representing the air-filled bronchi) or fluid bronchogram (echo-free avascular tubular structures representing fluid filled bronchi). On the other hand, the pleural criteria include a localized pleural effusion or a basal pleural effusion describing the pleural fluid which accumulates in the costophrenic angle (12).

For peripheral bronchogenic carcinomas, they usually appear as round or oval, sometimes polycyclic, hypoechoic lesion (13) with typically absent air bronchogram (13,14). Tumor necrosis can be seen as a particularly hypoechoic to anechoic region within the tumor (14). The previously described pneumonic consolidation and peripheral bronchogenic carcinoma were differentiated from compression atelectasis (discussed below as a consequence of space-occupying pleural effusion) as shown in Table 1. For central bronchogenic carcinoma, the distal atelectasis due to obstruction was identified (13) appearing more echogenic than the hypoechoic central obstructive tumor (15). Metastatic pulmonary nodules were considered when one or more pulmonary nodules was detected in a patient with a history of underlying malignancy as this is almost always suggestive of metastatic disease (16). The nodules were identified having round shape with typically clear borders and variable echotexture (14).

Concerning pleural abnormalities, the diagnostic criteria for pleural effusion included any of the following: demonstration of an anechoic space between the visceral and parietal pleura which varies during breathing (17), the presence of parenchymal atelectasis appearing in the form of a short lingula floating in an anechoic space (18) or visualization of echogenic particles and moving septa that move in an anechoic space (17). Sinusoid sign was also used indicating pleural effusion regardless of its echogenicity (1,5).

Alternatively, pneumothorax was diagnosed by absent lung sliding in combination with the A-line sign (only A-lines) as this constellation is very specific for pneumothorax (19). Furthermore, on M-mode, the normal granular pattern "sea-shore sign" is replaced by horizontal lines "stratosphere sign" which represent abolition of lung sliding (20). The lung point sign indicating the area in which the lung intermittently comes in contact with the chest wall during respiration (10) was

additionally used as it is 100% specific for pneumothorax (21). On the other hand, when local lung sliding or B-lines (lung rocket) was detected, diagnosis was excluded (20).

Hydropneumothorax was identified by visualization of air-fluid boundary which can move with respiration, absent sliding sign above the air-fluid level (22) and the "curtain sign" (reverberation artifacts originating from the air within the pleura obscuring the underlying effusion during inspiration) (23). Considering mesothelioma, it was diagnosed by demonstration of diffuse pleural thickening with accompanying pleural calcifications, pleural effusion and focal pleural mass (17).

2.5. Data analysis

A hemithorax was categorized as positive for an abnormality if it presented at least one positive region, while, it was categorized as negative if all regions were free of any abnormality. The results of chest US were compared with the corresponding chest MDCT findings using chest MDCT as the diagnostic standard of reference. The sensitivity, specificity, positive predictive value (PPV), negative predictive value (NPV) and diagnostic accuracy (DA) of chest US for each encountered pathological entity were calculated using standard formulas.

3. Results

The patients included in our study were 55 males and 35 females with mean age of 50 years and age range of 45–65 years. The provisional diagnoses with the patients' number are listed in Table 2. 180 hemithoraces (2 in each patient) were evaluated by chest US and chest CT. The sensitivity, specificity, PPV, NPV and DA of chest US for each encountered pathological entity were calculated using standard formulas as shown in Table 3.

Chest US had one false negative result for pneumothorax, two false negative results for bronchogenic carcinomas and three false positive results for pneumonic consolidation. Thus, the sensitivity, specificity, PPV, NPV and DA of chest US were 92%, 100%, 100%, 99% and 99% for pneumothorax, 71%, 100%, 100%, 98% and 98% for bronchogenic carcinoma and 100%, 96%, 84%, 100% and 97% for pneumonic consolidation respectively. Conversely, chest US did not have any false positive or false negative results throughout the rest of the abnormalities included in our study. Therefore, the values of the sensitivity, specificity, PPV, NPV and DA of chest US were 100% for metastatic pulmonary nodules, pleural effusion, hydropneumothorax and mesothelioma.

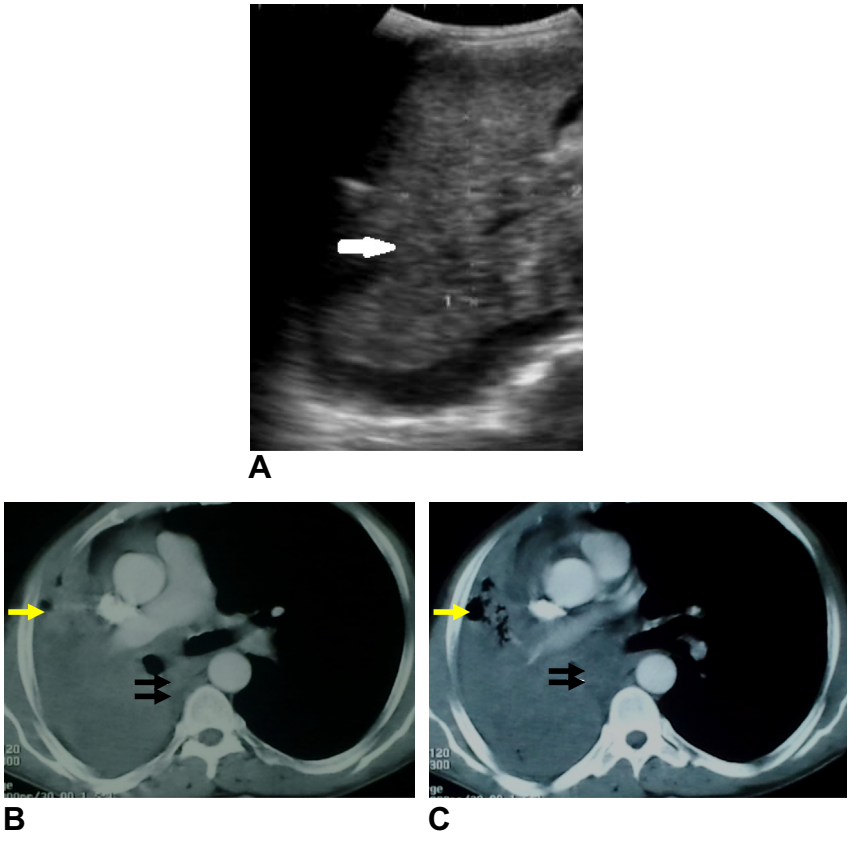

Fig. 3 (A) Chest US image in B-mode clearly demonstrates a central obstructive mass appearing slightly hypoechoic (arrowed) in comparison to the more echogenic distal lung consolidation. (B and C) Postcontrast chest CT axial images in mediastinal window settings show a small right-sided perihilar soft tissue attenuation mass (black arrows) with abrupt bronchial termination and distal consolidation lung collapse. A note is made of the positive air bronchogram in the consolidated collapsed right lung (yellow arrows) and compensatory emphysematous changes of the left lung. Histopathology revealed non-small cell lung carcinoma.

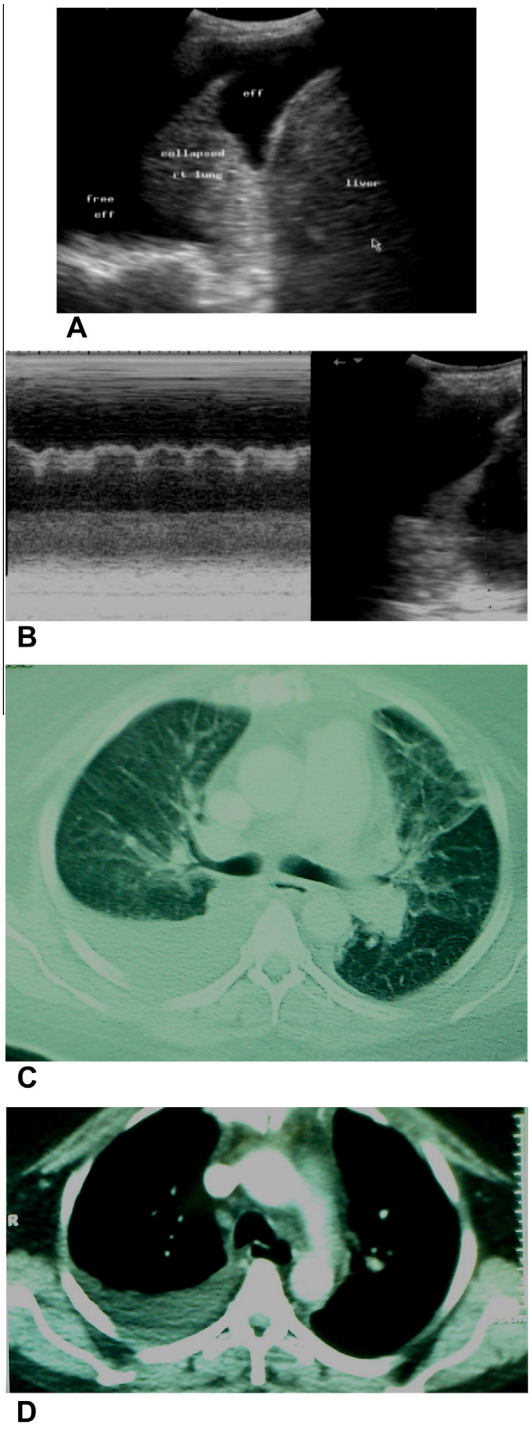

Fig. 4 (A) Chest US image in B-mode shows an anechoic right-sided pleural effusion which is abundant enough to be compressive with the atelectatic underlying right lung. The atelectatic underlying right lung is seen as consolidated appearing of liver-like echogenicity and floating in the pleural effusion. (B) Chest US image in M-mode displays the sinusoidal sign which represents the undulating movements of the lung and visceral pleura in the pleural effusion. (C and D) Postcontrast chest CT axial images in lung (C) and mediastinal (D) window settings display right-sided, crescent-shaped, posterior and basal pleural effusion (free effusion) with partial compression collapse of the underlying lower lung lobe.

Consequently, chest US exhibited high overall sensitivity, specificity and diagnostic accuracy for all pleural and pulmonary pathologies. Therefore, chest US was performed well in detection of various pleural and pulmonary diseases among the patients enrolled in this study.

4. Discussion

Although, it is entrenched that portable CXR is the most commonly requested radiographic examination (24), limitations of portable CXR have been well described and lead to poor quality X-ray films with low sensitivity. Moreover, it has been shown that even under carefully controlled exposure conditions more than 30% of the X-ray films are considered suboptimal (25).

In this study, we evaluated chest US as an individual variable and we did not use chest radiography purposely for interpretation in various pathological entities whether pulmonary or pleural in a group of ICU patients. For the reason that some CXR were inevitably of poor value and low sensitivity with those ICU patients for whom supine portable radiographs were taken. The concerned pulmonary entities included pneumonic consolidation, bronchogenic carcinoma and metastatic pulmonary nodules. On the other hand, the concerned pleural entities included pleural effusion, pneumothorax, hydropneumothorax and mesothelioma. We selected these various pathological entities as they had important implications in patient's management. Moreover, physicians in ICU are cornered by the bad patient's general condition that may hinder further patient's transfer. This is in addition to the low availability of the investigations that could help to reach disease diagnosis. Therein, we intended to evaluate the diagnostic performance of chest US, as a simple and widely available bedside tool, by accurate examination of all lung regions in each patient and by comparing these findings with the findings of chest MDCT using chest MDCT as the diagnostic standard of reference.

In the current study, identification of normal lung was made by visualization of lung sliding and A-lines. These are in addition to B-lines and the seashore sign on M-mode (the equivalent of lung sliding) (Fig. 1). Alternatively, we identified pneumonic consolidation as we were attentive of the patient's clinical history and by using the parenchymal and pleural criteria with a corresponding sensitivity of 100%. These are compared to the results of the study performed by Shah et al. (26) as US had an overall sensitivity of 86%, specificity of 89% for diagnosing pneumonia by visualizing lung consolidation with sonographic air bronchogram. Additionally, detection of pneumonic consolidation by chest US in our study was strongly correlated with its presence on chest CT as shown in Fig. 2. However, chest US had three false positive cases resulting in a specificity of 96%. These false positive results may be attributed to the time interval between chest US and chest MDCT (up to 24 h). This is in addition to the patient's mobilization and transportation which in turn may result in resolution of small- sized pneumonic consolidation particularly in mechanically ventilated patients.

In identifying bronchogenic carcinomas, chest US had a sensitivity, specificity and diagnostic accuracy of 71%, 100% and 98% respectively. For central lung tumors, it was found that US can distinguish between atelectasis and a central mass

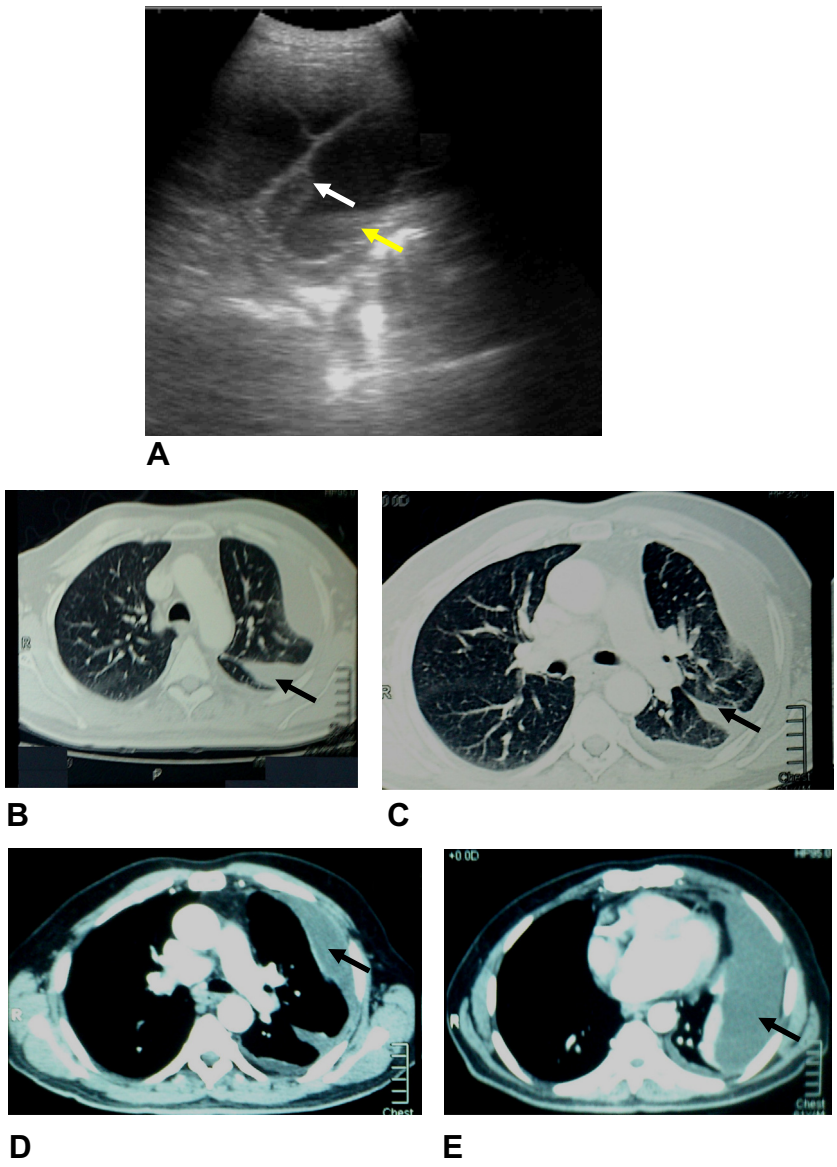

Fig. 5 (A) Chest US in B-mode shows a moderate amount of encysted pleural effusion which is associated with marked pleural thickening. The dependent part of the effusion shows increased echogenicity (yellow arrow) with thick septations (white arrow) inside. These ultrasonographic findings are keeping with complex septated type of effusion. (B–E) The corresponding chest CT axial images in lung (B and C) and mediastinal (D and E) window settings display moderate amount of left-sided encysted pleural effusion (arrowed) with partial compression collapse of the underlying lung parenchyma. Biochemistry confirmed the suspected exudative nature of the effusion.

in 50% of cases (27). Also, chest US in this study failed to diagnose two patients in comparison to chest CT and successively diagnosed the remaining patients through demonstration of the hypoechoic central obstructive tumor and the more echogenic distal consolidation as shown in Fig. 3. On the other hand, we detected peripheral lung tumors well by chest US through detection of absent echogenic line of the visceral pleura where the tumor abuts the pleura with posterior acoustic enhancement and typically absent air bronchogram. The typically absent air bronchogram is explained as solid carcinomas do not contain aerated lung parenchyma (13,14). Furthermore, chest US detected all patients with metastatic pulmonary nodules in our study. Chest US enables one to visualize even small peripheral metastatic lesions (28), though; CT is the most accurate imaging modality for detecting nodules over the entire lung (16).

Wang and Doelken (10) asserted that the use of pleural US in the critically ill patients allows earlier and more frequent assessment as well as more accurate characterization of pleural disease than standard CXR combined with physical examination. In our study, chest US had a sensitivity and specificity of 100% for detection of pleural effusion in proportion to sensitivity of 100% and specificity of 99.7% obtained by other researchers (29). In this study, we identified the four displays of pleural effusion described by Rumende (17) according to its internal echogenicity; (a) anechoic (Fig. 4), (b) complex

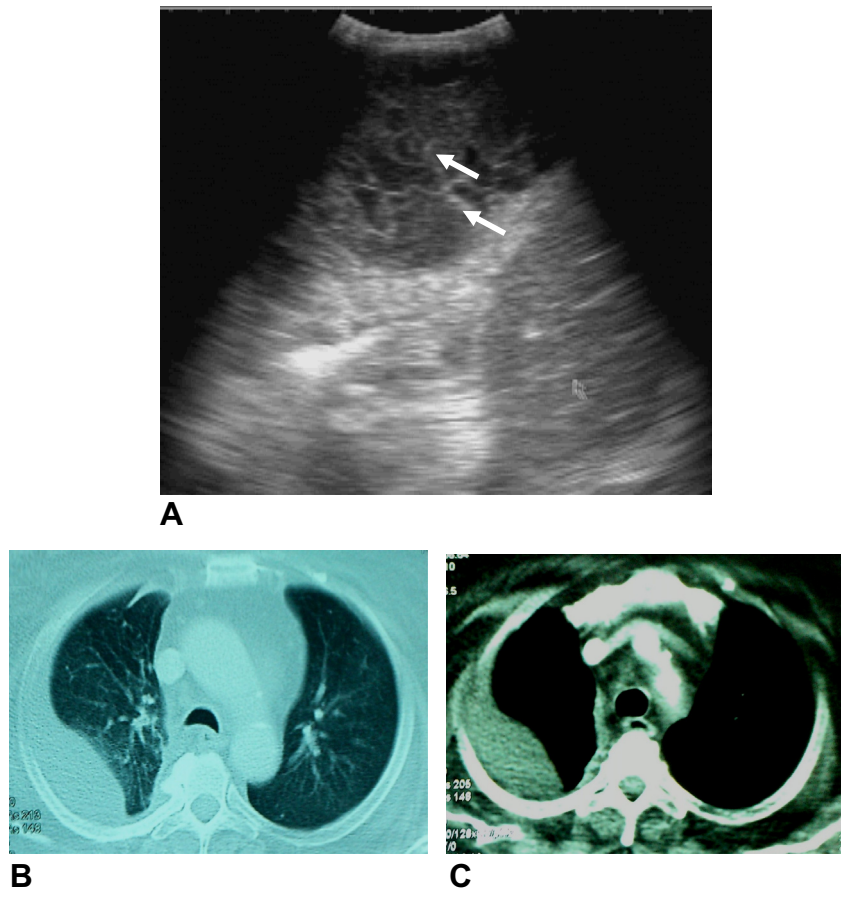

Fig. 6 (A) Chest US image in B-mode shows moderate amount of highly echogenic right-sided encysted pleural effusion with fine internal septations (arrowed). (B and C) Postcontrast chest CT images in lung (B) and mediastinal (C) window settings display moderate amount of right-sided encysted pleural effusion, however, the fine septations seen by chest US were not evident by CT.

non-septated (multiple internal echoes in the dependent part of the effusion), (c) complex septated (Fig. 5) and (d) homogenously echogenic. Moreover, chest US has been shown to be more sensitive than CT in demonstrating the presence of septa inside a pleural effusion (30) as shown in Fig. 6. The presence of septa has several implications. Chen et al. (31) demonstrated that patients with septated effusions needed longer chest tube drainage and longer hospital care and were more likely to require fibrinolytic therapy or surgery compared with those with unseptated effusions. Tu et al. (32) also confirmed some of these findings in medical intensive care unit patients. In our study, chest US clearly showed fine internal septations in seven patients out of the twelve patients with encysted pleural effusion. This significant finding was reflected on their further management as two of them received intrapleural fibrinolytic therapy.

It is well known that pneumothorax is a frequently entertained diagnosis in the ICU (33). Its bedside diagnosis is extremely important in ICU patients (20). Chest CT has become the gold standard for this purpose inspite of having inherent problems of time lag, transportation and radiation exposure. US is comparable to CT in the evaluation of pneumothorax in the ICU patient (33). In this study, chest US has been successfully used for the identification of pneumothorax in a variety of patients (Fig. 7) but had only one false negative result. Thus, a sensitivity of 92% and a specificity of 100% were obtained. This is comparable to a sensitivity of 86% and a specificity of 97% in the study performed by Zhang et al. (34).

The only case of pneumothorax missed by chest US in our study was small in size and did not require drainage corresponding to the result of the study performed by Brook et al. (35). Therefore, in this study, chest US did not miss any clinically significant pneumothorax and is considered a reliable bedside tool to diagnosis such abnormality. We used absent lung sliding with the A-line sign and the lung point sign to specifically diagnose pneumothorax, thus, no false positive results were obtained. This is different from another study which had five false positive pneumothoraces (3) as the lung point sign was not used in that study to specifically diagnose pneumothorax.

Regarding patients with hydropneumothorax, chest US successfully diagnosed all patients as US can recognize pneumothorax more easily by identifying the air-fluid boundary (22). Moreover, others ascertained that the "curtain sign"

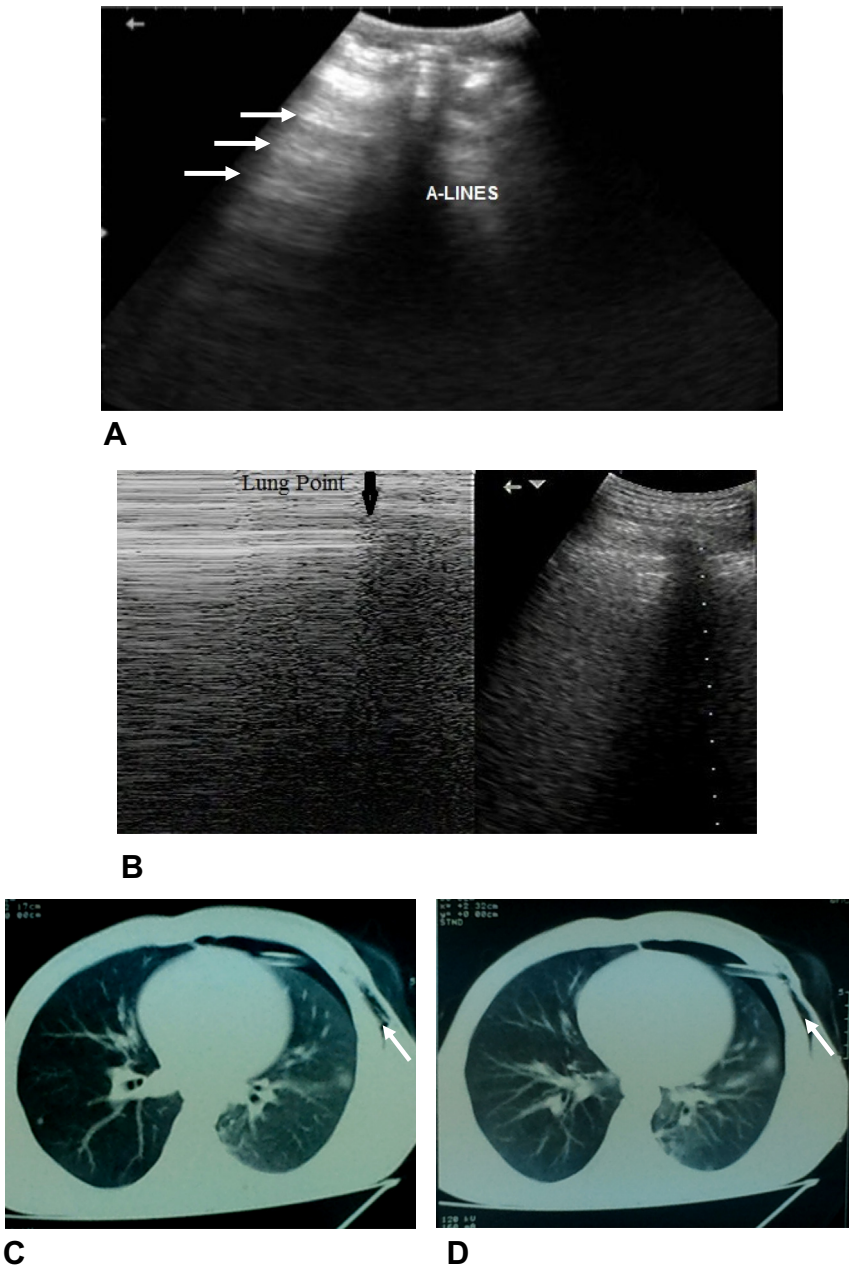

Fig. 7 (A) Chest US image in B-mode displays a multitude of exaggerated horizontal reverberation artifacts (A-lines) (arrowed) seen in the form of echogenic lines parallel to the pleural surface and equidistant from each other. (B) Chest US image in M-mode reveals the lung point sign (arrowed) which is the transition point between strictly horizontal lines (the so-called ''stratosphere sign'') and the normal granular pattern (the so-called ''seashore sign''). (C and D) Postcontrast chest CT images in lung window settings display mild left-sided pneumothorax with partial compression collapse of the underlying lung and an intercostal tube seen in situ with surgical emphysema along the left lateral chest wall (arrowed).

allows a confident diagnosis to be made (23). Similarly, chest US diagnosed all patients with pathologically proven mesothelioma (Fig. 8) as it is well known that US can readily distinguish between pleural fluid and thickening (36). With US, an area of abnormal pleura can be localized which makes yield of the targeted biopsy greater than random pleural sampling (37). In addition, the entry of medical thoracoscopy into the hemithorax can be avoided with the use of US in a case suspicious for mesothelioma to evade tumor seeding (36).

To conclude, chest ultrasonography exhibited higher overall sensitivity, specificity and diagnostic accuracy for all concerned pleural and pulmonary pathologies. Consequently, chest ultrasonography can be adjoined in the up-to-date work-up of the ICU setting as an ancillary bedside tool aiding in disease diagnosis.

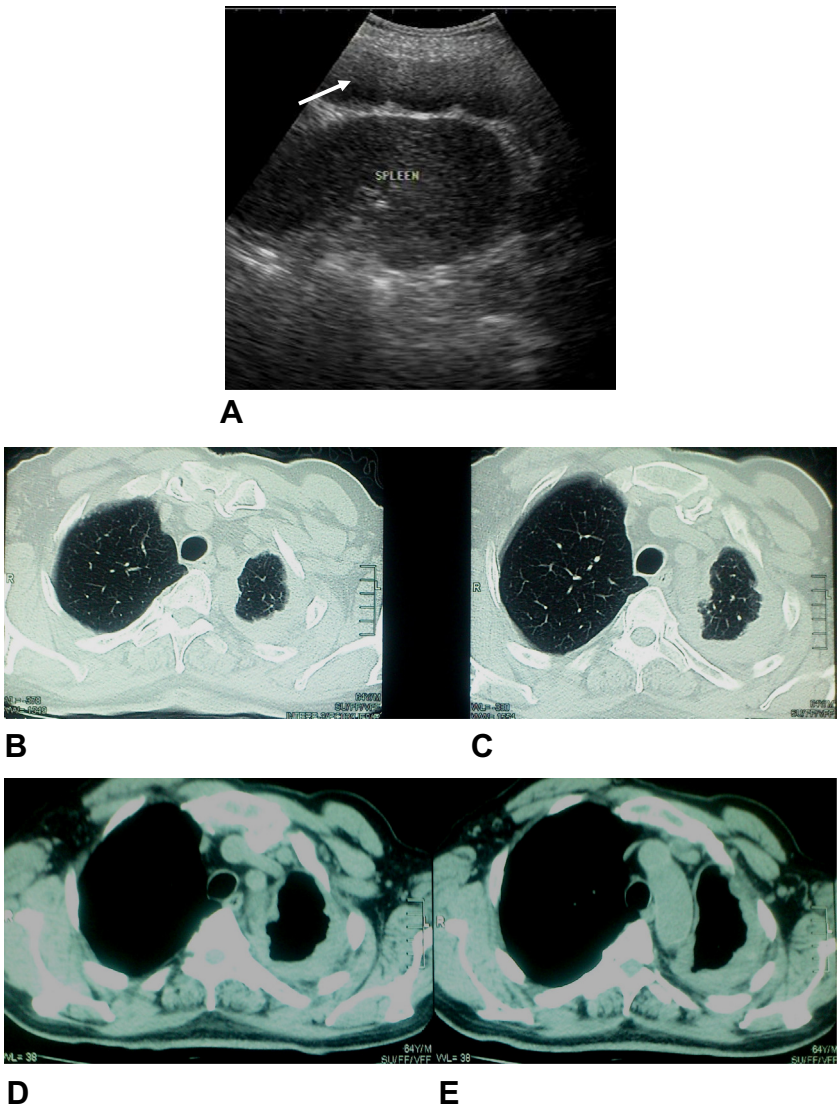

Fig. 8 (A) Chest US image in B-mode displays a hypoechoic band of continuous pleural thickening involving the left diaphragmatic pleura (arrowed). (B–E) Postcontrast chest CT images in lung (B and C) and mediastinal (D and E) window settings display lobulated circumferential left pleural thickening which involves the mediastinal and costal pleural surfaces with volume loss of the underlying lung. The patient was pathologically proven to have pleural mesothelioma.

Conflict of interest

None.

References

(1) Bouhemad B, Zhang M, Lu Q, et al. Clinical review: bedside lung ultrasound in critical care practice. Crit Care 2007;11(1):205.
(2) Gardelli G, Feletti F, Nanni A, et al. Chest ultrasonography in the ICU. Respir Care 2012;57(5):773–81.
(3) Xirouchaki N, Magkanas E, Vaporidi K, et al. Lung ultrasound in critically ill patients: comparison with bedside chest radiography. Intensive Care Med 2011;37(9):1488–93.
(4) Peris A, Tutino L, Zagli G, et al. The use of point-of-care bedside lung ultrasound significantly reduces the number of radiographs and computed tomography scans in critically ill patients. Anesth Analg 2010;111(3):687–92.
(5) Lichtenstein DA, Mezière GA. Relevance of lung ultrasound in the diagnosis of acute respiratory failure: the BLUE protocol. Chest 2008;134(1):117–25.
(6) Soldati G, Sher S. Bedside lung ultrasound in critical care practice. Minerva Anestesiol 2009;75(9):509–17.
(7) Koenig SJ, Narasimhan M, Mayo PH. Thoracic ultrasonography for the pulmonary specialist. Chest 2011;140(5):1332–41.
(8) Ashton-Cleary DT. Is thoracic ultrasound a viable alternative to conventional imaging in the critical care setting? Br J Anaesth 2013;111(2):152–60.
(9) Hansell DM, Bankier AA, MacMahon H, et al. Fleischner Society: glossary of terms for thoracic imaging. Radiology 2008;246(3):697–722.
(10) Wang JS, Doelken P. Pleural ultrasonography in the intensive care unit. In: Bolliger CT, Herth FJF, Mayo PH, et al., editors. Clinical chest ultrasound: from the ICU to the bronchoscopy suite. Progress in respiratory research. Basel: Karger; 2009. p. 82–8.

(11) Pellecchiaa C, Mayo PH. Ultrasound evaluation of the lung. In: Bolliger CT, Herth FJF, Mayo PH, et al., editors. Clinical chest ultrasound: from the ICU to the bronchoscopy suite. Progress in respiratory research. Basel: Karger; 2009. p. 76–81.
(12) Reissig A, Kroegel C. Diagnosis of pulmonary embolism and pneumonia using transthoracic sonography. In: Bolliger CT, Herth FJF, Mayo PH, et al., editors. Clinical chest ultrasound: from the ICU to the bronchoscopy suite. Progress in respiratory research. Basel: Karger; 2009. p. 43–50.
(13) Beckh S, Bölcskei PL, Lessnau KD. Real-time chest ultrasonography: a comprehensive review for the pulmonologist. Chest 2002;122(5):1759–73.
(14) Reissig A, Görg C, Mathis G. Transthoracic sonography in the diagnosis of pulmonary diseases: a systematic approach. Ultraschall Med 2009;30(5):438–54, quiz 455–56.
(15) Yang PC, Luh KT, Wu HD, et al. Lung tumors associated with obstructive pneumonitis: US studies. Radiology 1990;174(3 Pt 1): 717–20.
(16) Webb RR. Radiologic evaluation of the solitary pulmonary nodule. AJR 1990;154(4):701–8.
(17) Rumende CM. The role of ultrasonography in the management of lung and pleural diseases. Acta Med Indones 2012;44(2):175–83.
(18) Mayo PH, Goltz HR, Tafreshi M, et al. Safety of ultrasound-guided thoracentesis in patients receiving mechanical ventilation. Chest 2004;125(3):1059–62.
(19) Chandra S, Narasimhan M. Pleural ultrasonography. Open Crit Care Med J 2010;3(2):26–32.
(20) Lichtenstein DA, Mezière G, Lascols N, et al. Ultrasound diagnosis of occult pneumothorax. Crit Care Med 2005;33(6): 1231–8.
(21) Lichtenstein D, Mezière G, Biderman P, et al. The lung point: an ultrasound sign specific to pneumothorax. Intensive Care Med 2000;26(10):1434–40.
(22) Targhetta R, Bourgeois JM, Chavagneux R, et al. Ultrasonographic approach to diagnosing hydropneumothorax. Chest 1992; 101(4):931–4.
(23) Koh DM, Burke S, Davis N, et al. Transthoracic US of the chest: clinical uses and applications. Radiographics 2002;22(1):e1.
(24) Rubinowitz AN, Siegel MD, Tocino I. Thoracic imaging in the ICU. Crit Care Clin 2007;23(3):539–73.
(25) Henschke CI, Yankelevitz DF, Wand A, et al. Accuracy and efficacy of chest radiography in the intensive care unit. Radiol Clin North Am 1996;34(1):21–31.
(26) Shah VP, Tunik MG, Tsung JW. Prospective evaluation of point-of-care ultrasonography for the diagnosis of pneumonia in children and young adults. JAMA Pediatr 2013;167(2):119–25.
(27) Görg C, Weide R, Schwerk WB. Sonographische befunde bei ausedehnten lungenatelektasen. Ultraschall Klin Prax 1996;11: 14–9.
(28) Sartori S, Tombesi P. Emerging roles for transthoracic ultrasonography in pleuropulmonary pathology. World J Radiol 2010; 2(2):83–90.
(29) Gryminski J, Krakówka P, Lypacewicz G. The diagnosis of pleural effusion by ultrasonic and radiologic techniques. Chest 1976;70(1):33–7.
(30) Riccabona M. Ultrasound of the chest in children (mediastinum excluded). Eur Radiol 2008;18(2):390–9.
(31) Chen KY, Liaw YS, Wang HC, et al. Sonographic septation: a useful prognostic indicator of acute thoracic empyema. J Ultrasound Med 2000;19(12):837–43.
(32) Tu CY, Hsu WH, Hsia TC, et al. Pleural effusions in febrile medical ICU patients: chest ultrasound study. Chest 2004;126(4): 1274–80.
(33) Rankine JJ, Thomas AN, Fluechter D. Diagnosis of pneumothorax in critically ill adults. Postgrad Med J 2000;76(897): 399–404.
(34) Zhang M, Liu ZH, Yang JX, et al. Rapid detection of pneumothorax by ultrasonography in patients with multiple trauma. Crit Care 2006;10(4):R112.
(35) Brook OR, Beck-Razi N, Abadi S, et al. Sonographic detection of pneumothorax by radiology residents as part of extended focused assessment with sonography for trauma. J Ultrasound Med 2009;28(6):749–55.
(36) Michaud G, Ernst A. Ultrasound and medical thoracoscopy. In: Bolliger CT, Herth FJF, Mayo PH, et al., editors. Clinical chest ultrasound: from the ICU to the bronchoscopy suite. Progress in respiratory research. Basel: Karger; 2009. p. 182–8.
(37) Diacon AH, Theron J, Schubert P, et al. Ultrasound assisted transthoracic biopsy: fine-needle aspiration or cutting-needle biopsy? Eur Respir J 2007;29(2):357–62.